

AD-A118 734

AIR FORCE GEOPHYSICS LAB HANSCOM AFB MA
THE STATISTICAL RELATIONS AMONG Q, KP, AND THE GLOBAL WEATHER C--ETC(U)

F/G 8/14

JAN 82 B S DANDEKAR

AEGL-TR-82-0010

NL

UNCLASSIFIED

1 OF 1
40 A
00734

END
DATE FILMED
09-82
DTIC

ED A

AD A118734

AFGL-TR-82-0010
ENVIRONMENTAL RESEARCH PAPERS, NO. 763



12

The Statistical Relations Among Q, K_p, and the Global Weather Central - K Indices

B. S. DANDEKAR

13 January 1982



Approved for public release; distribution unlimited.

DRC FILE COPY

SPACE PHYSICS DIVISION
AIR FORCE GEOPHYSICS LABORATORY
HANSCOM AFB, MASSACHUSETTS 01731

PROJECT 414L

AIR FORCE SYSTEMS COMMAND, USAF



Unclassified

SECURITY CLASSIFICATION OF THIS PAGE (When Data Entered)

REPORT DOCUMENTATION PAGE		READ INSTRUCTIONS BEFORE COMPLETING FORM
1 REPORT NUMBER AFGL-TR-82-0010	2 GOVT ACCESSION NO. <i>AD-A118734</i>	3 RECIPIENT'S CATALOG NUMBER
4 TITLE (and Subtitle) THE STATISTICAL RELATIONS AMONG Q, Kp, AND THE GLOBAL WEATHER CENTRAL -K INDICES		5 TYPE OF REPORT & PERIOD COVERED Scientific. Interim.
7 AUTHOR(s) B.S. Dandekar		6 PERFORMING ORG. REPORT NUMBER ERP No. 763
9 PERFORMING ORGANIZATION NAME AND ADDRESS Air Force Geophysics Laboratory (PHY) Hanscom AFB Massachusetts 01731		10 PROGRAM ELEMENT, PROJECT, TASK AREA & WORK UNIT NUMBERS 62101F 414L0101
11 CONTROLLING OFFICE NAME AND ADDRESS Air Force Geophysics Laboratory (PHY) Hanscom AFB Massachusetts 01731		12 REPORT DATE 13 January 1982
14 MONITORING AGENCY NAME & ADDRESS (if different from Controlling Office)		13 NUMBER OF PAGES 33
16 DISTRIBUTION STATEMENT (of this Report) Approved for public release; distribution unlimited.		15 SECURITY CLASS. (or this report) Unclassified
17 DISTRIBUTION STATEMENT (of the abstract entered in Block 20, if different from Report)		15a DECLASSIFICATION/DOWNGRADING SCHEDULE
18 SUPPLEMENTARY NOTES		
19 KEY WORDS (Continue on reverse side if necessary and identify by block number) Magnetic activity index Auroral oval Auroral ionospheric disturbances		
20 ABSTRACT (Continue on reverse side if necessary and identify by block number) The K index determined by the Air Force Global Weather Central has been compared with Kp and Q (from Sodankyla) for the period March 1978 – May 1981 to determine empirical relations between Kp vs K, Q vs Kp, and Q vs K. The study shows that the K index is a reasonably good measure of Kp during most of the time. The time-dependent relations between Q and K, and Kp and K are derived, so that one can convert the K (AFGWC) index to the Kp or Q index for specification of the auroral ionosphere in the Experimental Radar System test region. Appendix A presents the relation between Q, Kp		

DD FORM 1 JAN 73 1473

Unclassified

SECURITY CLASSIFICATION OF THIS PAGE (When Data Entered)

Unclassified

SECURITY CLASSIFICATION OF THIS PAGE(When Data Entered)

20. Abstract (Continued)

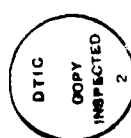
and the diffuse (continuous) aurora. Appendix B discusses the relation between Q and K_p using a 4-year data base.

Unclassified

SECURITY CLASSIFICATION OF THIS PAGE(When Data Entered)

Preface

The author thanks the Air Force Global Weather Central (AFGWC), Offutt AFB, Nebraska for providing the GWC K-index data. The author is also thankful to Mr. J. Buchau (for many useful suggestions) and Col. R. Thompson for their interest in the work.



3

Accession For	
NTIS GRA&I	
DTIC TAB	
Unannounced	
Justification	
By _____	
Distribution/	
Availability Code	
Dist	Avail and/or Special

A large checkmark is present above the "Justification" line. A handwritten mark resembling a signature is written across the bottom right corner of the form.

Contents

1. INTRODUCTION	7
2. DATA BASE	8
3. ANALYSIS	9
4. CONCLUSIONS	22
REFERENCES	25
APPENDIX A: Determination of Q (or Kp) From Photometric Auroral Observations	27
APPENDIX B: Relationship Between Kp and Q _{SOD}	31

Illustrations

1. Location of the Q = 3 Feldstein Oval with Respect to Sodankyla at 08 and 22 UT	11
2. Magnetometer Network for K and Kp in Corrected Geomagnetic Coordinates	12
3. Diurnal Variation of Kp, K, and Q Indices	15
4. Dependence of the Correlation on UT for (a) Kp vs K, (b) K vs Q, (c) Kp vs Q	18
5. Dependence of Multiplication Factors (Slope) on UT for (a) Kp vs K, (b) K vs Q, (c) Kp vs Q	19

Illustrations

6. Relations Between K _p and K for 06-09 UT and 18-21 UT Intervals	21
A1. Location of Equatorward Edge of Aurora vs K _p and Q Indices	29
A2. Relations Among Magnetic Activity Levels and Auroral Locations	30

Tables

1. Distribution of K Data with Respect to K _p Data	10
2. Magnetometer Stations for K _p , K, and Q Indices	14
3. Summary of Correlation Analysis	16
4. Empirical Time Dependent Factors for Conversion of K to Q	22
B1. Relationship Between K _p and Q _{SOD}	32

The Statistical Relations Among Q, K_p, and the Global Weather Central -K Indices

I. INTRODUCTION

In the geographical region covered by the Over-the-Horizon (OTH) Experimental Radar System, the auroral ionosphere is one of the most important environmental factors affecting the performance of the radar. It is known that the high latitude ionosphere and the auroral oval are best ordered by the high latitude magnetic activity index Q. The diameter of the auroral oval and its location are best expressed in terms of the Q index. On the other hand, high latitude ionospheric phenomena have been expressed as a function of global geomagnetic activity using the K_p index. Therefore, to provide the future Operational Radar System with specifications of the auroral and sub-auroral (F-trough) ionosphere, it is important to have Q and K_p indices, or other equivalent parameters, available in real time.

Ideally, the Q index is determined by a measurement on the midnight magnetic meridian at a geomagnetic latitude $\Lambda \geq 58^{\circ}$. At present, the Q index is measured at only one station, Sodankyla, Finland.

The Q index measured at a single station shows a typical diurnal variation¹ due to the movement of the station with respect to the auroral oval (explained in the analysis section). This systematic diurnal variation prevents the use of a

(Received for publication 11 January 1982)

1. Dandekar, B.S. (1979) Magnetic Disturbance Statistics from a Single Station Q Index Applied to an Actual OTH-B Radar Situation, AFGL-TR-79-0296, AD A084 808.

single-station Q index to specify the position of the auroral oval at all Universal Times. The planetary index of magnetic activity K_p can be used to specify the position of the auroral oval. However, a delay averaging 2 months occurs before the K_p index becomes available, which prevents the use of the K_p index for real time prediction or specification of the auroral oval.

Because no index of global magnetic activity is available on a real-time basis, the Air Force Global Weather Central (AFGWC) relies on a determination of a 3-hourly K index computed from the magnetic observations from five observatories. A preliminary analysis² based on a small sample of data from 4 months (June-October 1980), showed the feasibility of using the AFGWC K index in deriving Q (or K_p) required for the specification of the auroral ionosphere. This report presents the results from a much wider data base of 39 months. For convenience, the AFGWC K index will be referred to simply as the K index.

The study showed that the K index tracks the K_p index fairly well. However, the K index has some shortcomings: For low values of K_p the K index is 1/3 unit larger than the K_p index; for high values of K_p, the K index is 1/3 unit smaller than the K_p index; and since small values of K and K_p are more common, the K index is 1/3 unit larger than the K_p index for most values measured. In addition, the K index exhibits some diurnal variation. Empirical, time dependent factors have been determined to correct K so that it more closely corresponds to K_p. Also, empirical relations between K, K_p, and Q have been determined for obtaining the Q index from K.

2. DATA BASE

The AFGWC K-index data for March 1978-May 1981 were used in this study. The K_p index and the Q index from Sodankyla were also used in the analysis. The latter data sets are from the World Data Center A, Boulder, Colorado.

Instead of the conventional quasilogarithmic K index, AFGWC provided the linear ap index. These data were converted to the AFGWC K indices.³ In the following analysis it is assumed that all these data have been properly scaled and need no correction for observational procedures.

During the period of 39 months, AFGWC implemented several changes in the K-index network operation. Therefore the data were initially divided into four corresponding separate sets for analysis. Since no significant differences were

2. Dandekar, B. S. (1979) Study of the Equatorward Edge of the Auroral Oval from Satellite Observations, AFGL-TR-79-0010, AD A072 997.
3. Prochaska, R. D., Capt., Geomagnetic Index Calculation and Use at AFGWC, AFGWC/Tn-80/002.

found among the separate data sets, all the data were treated as a single continuous set in the following analysis.

3. ANALYSIS

The averaged K determined for all data taken for a particular Kp level should correspond exactly to that particular K. A measure of the quality of the K index is how well K matches Kp for a selected Kp level and the standard deviation σ of the respective K distribution. A large σ indicates the data base may be too small for K to systematically produce a reliable Kp estimation. A systematic difference between average K and Kp would suggest a weighting error of the input (station) K values, or neglect of possible diurnal variations emphasized by the small longitude sector (see Figure 2, which is shown later) providing inputs to K, to systematically produce a reliable Kp estimation.

All this can be tested by the mass plot of the data. In practice, the fixed intervals for the indices combined with the large number of data points results in a thick superposition of about 150 separate points. This limitation can be bypassed by studying the observed frequency distributions of the observations in the corresponding intervals of K and Kp. This distribution is presented in Table 1. In Table 1 the observed frequencies in the Kp intervals are along the columns and the frequencies in the K intervals are along the rows. The sum of the occurrence frequencies along the row is in the last column, and the sum down the column is in the bottom row.

In Table 1, the lowest value $K = 0_0$ (last column, row 1, summation frequency = 0) is absent. The corresponding lowest value $Kp = 0_0$ is seen 139 times (in the first column and last row). The highest value $Kp = 8_+$ corresponds to the highest value $K = 9_0$. The median range (50 percent of the observations) of $Kp = 2_0$ corresponds to $K = 2_+$. The highest observed frequency of Kp is between 2_+ and 3_- , whereas the corresponding range of K is 2_- to 2_+ . The results show that K is a reasonably good, but not identical, replacement for the Kp index.

To determine the correlation between K and Kp, a least squares straight line was fitted between K and Kp. It is known that the equation for the least squares straight line fit is not necessarily reversible.⁴ Therefore, an average of the two straight line fits ($y = mx + c$ and $x = m'y + c'$) is given here.

$$Kp = 1.09K - 0.43 \quad (1)$$

4. Spiegel, M. R. (1969) Theory and Problems of Statistics, Schaum Publishing Co., New York, p. 229.

Table 1. Distribution of the AFGWC-K Index with Respect to the Kp Index

Kp	0	0+	1-	1 ₀	1 ₊	2-	2 ₀	2 ₊	3-	3 ₀	3 ₊	4-	4 ₀	4 ₊	5-	5 ₀	5 ₊	6-	6 ₀	6 ₊	7-	7 ₀	7 ₊	8-	8 ₀	8 ₊	Total
0 ₀	0	52	50	39	14	14	4	2	3	2	2	1	1	1	1	1	1	1	1	1	1	1	1	1	1	184	
0 ₊	1	44	119	135	124	67	49	27	10	3	1	3	1	1	1	1	1	1	1	1	1	1	1	1	1	578	
1 ₋	1	210	92	125	127	68	78	57	13	8	4	3	3	1	1	1	1	1	1	1	1	1	1	1	1	629	
1 ₀	1	12	62	105	150	118	130	69	57	9	6	2	1	1	1	1	1	1	1	1	1	1	1	1	1	729	
1 ₊	2	6	44	76	125	148	129	105	83	49	11	5	1	1	1	1	1	1	1	1	1	1	1	1	1	780	
2 ₋	2	23	67	85	110	113	93	81	54	27	11	1	3	1	1	1	1	1	1	1	1	1	1	1	1	670	
2 ₊	2	24	43	112	141	182	208	200	149	77	28	6	2	4	1	1	1	1	1	1	1	1	1	1	1	1171	
3 ₋	3	7	30	58	73	108	184	239	218	162	108	33	8	5	2	2	2	2	2	2	2	2	2	2	2	1226	
3 ₀	3	2	5	10	20	42	59	129	151	160	106	69	36	8	3	1	1	1	1	1	1	1	1	1	1	783	
3 ₊	1	3	5	4	16	24	55	99	101	126	86	37	19	10	2	1	1	1	1	1	1	1	1	1	1	589	
4 ₋	2	1	1	3	6	14	24	32	86	115	80	73	37	21	4	2	1	1	1	1	1	1	1	1	1	522	
4 ₀	4	3	2	2	8	11	21	41	81	86	64	46	27	19	4	2	2	2	2	2	2	2	2	2	420		
4 ₊	3	3	2	3	3	5	20	39	49	59	31	32	14	7	4	3	3	3	3	3	3	3	3	3	294		
5 ₋	2	1	1	5	3	9	13	31	56	57	42	38	16	10	5	3	1	1	1	1	1	1	1	1	292		
5 ₀	2	2	3	3	1	1	4	15	16	28	32	27	21	22	9	4	1	3	1	3	1	3	1	3	196		
5 ₊	1	1	2	1	1	1	1	2	6	7	17	16	18	11	7	4	5	2	1	1	1	1	1	1	102		
6 ₋	1	1	1	1	1	2	2	6	8	7	13	14	9	11	3	1	1	1	1	1	1	1	1	1	74		
6 ₀	6	1	1	2	1	1	1	1	1	1	1	1	1	1	1	1	1	1	1	1	1	1	1	1	67		
6 ₊	7	1	2	1	1	1	1	1	1	1	1	1	1	1	1	1	1	1	1	1	1	1	1	1	35		
7 ₋	7	4	1	1	1	1	1	1	1	1	1	1	1	1	1	1	1	1	1	1	1	1	1	1	17		
7 ₀	8	1	1	1	1	1	1	1	1	1	1	1	1	1	1	1	1	1	1	1	1	1	1	1	1		
7 ₊	8	0	1	1	1	1	1	1	1	1	1	1	1	1	1	1	1	1	1	1	1	1	1	1	1		
Total	139	324	630	816	803	364	961	896	303	715	643	477	363	283	199	95	82	51	40	27	13	12	8	3	9392		

In Eq. (1) the slope is close to 1. The intercept is negative, showing that the value $K = 0_0$ does not correspond to $K_p = 0_0$. The standard deviation for the fit is 0.76. The correlation coefficient of 0.837 is high, showing a good agreement between K and K_p for 78 to 84 percent (0.837^2 to 0.837) of the data.

The magnitude of the slope and the high correlation coefficient show that K follows K_p very well. Before replacing K_p with K , one must look for the possible cause for the disagreement of about 30 percent of the data points.

For the study of the aurora, the quarter-hourly Q index for magnetic activity was suggested by Bartels in 1954. Bartels and Fukushima⁵ developed the scheme of determining the Q index. The Q index is determined from stations with geomagnetic latitudes higher than 58° . At present, only Sodankyla, Finland, measures the Q index.

A single-station Q index is known to exhibit a systematic diurnal variation¹ due to the towards-and-away movement of the station with respect to the aurora. This is shown schematically in Figure 1, in which the European sector is given in corrected geomagnetic coordinates. The double ring near the left hand bottom corner shows the CG pole. The horizontal line to the right is 90° CG longitude. The geographic North pole is marked "NP" in the figure. The oval rotates around the CG pole, while the station rotates around the North pole with the earth. The solid and dashed lines show the equatorward boundary of the Feldstein oval⁶ for $Q = 3$ at 22 and 08 UT respectively. The rotation of the earth brings Sodankyla, Finland ("SO" on the map) very close to the oval at 22 UT, and farthest away at 08 UT. The reliability of the Q index depends on the closeness of the oval to the station. Thus, the single-station Q index from Sodankyla is most reliable around 22 UT and is least reliable around 08 UT.

For this reason, mass plots between K_p (or K) and Q would be difficult to interpret. Therefore, such mass plots or frequency distributions are not presented in this analysis.

Differences in the geographic distribution of networks used to determine K and K_p might introduce systematic differences in the respective magnitudes of K and K_p . Similarly, a single-station Q index would generate different relations between K (or K_p) and the Q index, due to a systematic diurnal variation of the latter.¹

For operational systems, K is preferred to K_p because K is immediately available from the chain of magnetometer stations maintained by the Air Force Global Weather Central. The magnetometer stations used to determine the K_p and

5. Bartels, J., and Fukushima, N. (1956) Ein Q-Index für die Erdmagnetische Aktivität in Viertelstündlichen Intervallen, Abhandl. Akad. Wiss. Gottingen, Math-Phys. Klasse, Sonderheft-2.
6. Feldstein, Y.I. (1963) On the morphology of auroral and magnetic disturbances at high latitudes, Geomagn. Aeron. 3:183.

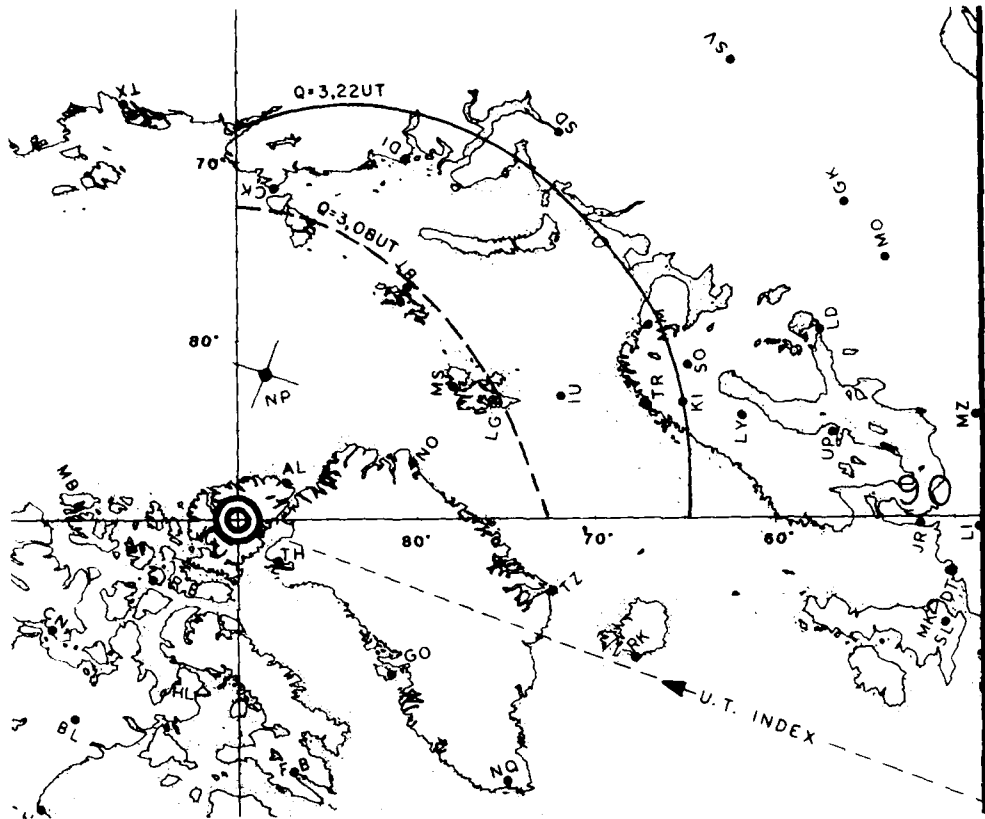


Figure 1. Location of the $Q = 3$ Feldstein Oval With Respect to Sodankyla at 08 and 22 UT

K indices respectively, are listed in Table 2. The distribution of magnetometer networks for K and K_p used by Prochaska³ is shown in Figure 2 (for station identification see Table 2) in corrected geomagnetic (CG) coordinates. A comparison of the distribution of stations used to determine K and K_p respectively, shows that in the 260°E - 20°E sector, the distribution is reasonable. However in the 70°E - 110°E sector, only one station measures K while seven stations measure K_p . These differences in locations and density of networks would contribute to some difference between K and K_p . Both the networks have no coverage over a wide longitude sector from 110°E to 250°E CG longitude.

To investigate any systematic differences between the diurnal variations of K and K_p , the average values for the 3-hour time intervals and their standard

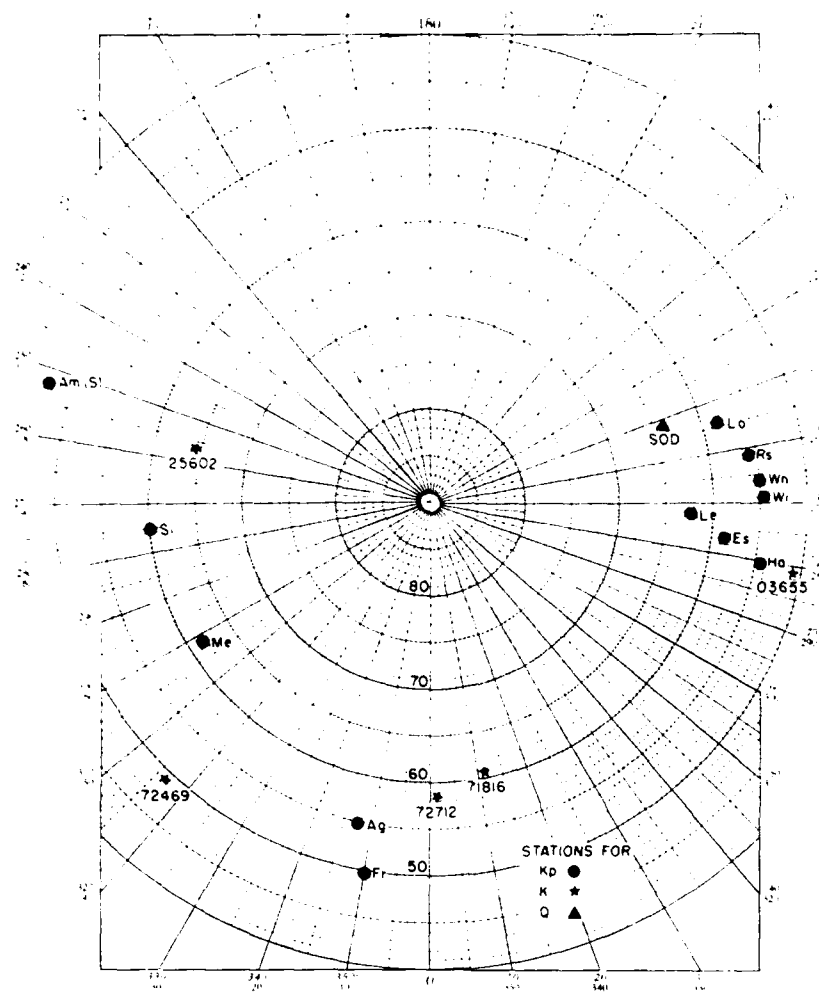


Figure 2. Magnetometer Network for K and Kp in Corrected Geomagnetic Coordinates

deviations are plotted in Figure 3. In Figure 3 the abscissa is UT and the ordinate is the index of magnetic activity. The variation of Kp is shown by solid lines whereas that of K is shown by dashed lines. For each interval three levels, corresponding to average $+\sigma$, average, and average $-\sigma$ respectively, are plotted. The figure shows that the diurnal variation in Kp is negligible, whereas the K index shows a significant diurnal variation. The figure shows that the difference in the diurnal variation of

Table 2. Magnetometer Stations for K_p, K and Q Indices*

Symbol	Observatory	Geographic		Geomagnetic	
		Lat	Long	Lat	Long
K_p Index					
Le	Lerwick, Shetland Islands	60 08N	358 49E	+62.5	88.6
Lo	Lovo, Sweden	59 21N	17 50E	+58.1	105.8
Si	Sitka, Alaska	57 04N	224 40E	+60.0	275.4
Rs	Rude Skov, Denmark	55 51N	12 27E	+55.8	98.5
Es	Eskdalemuir, Scotland	55 19N	356 48E	+58.5	82.9
Me	Mearook, Alberta, Canada	54 37N	246 40E	+61.8	301.0
Wn	Wingst, West Germany	53 45N	9 04E	+54.5	94.0
Wi	Witteveen, Netherlands	52 49N	6 40E	+54.2	91.0
Ha	Hartland, Devon, England	51 00N	355 31E	+54.6	79.0
Ag	Aigincourt, Ontario, Canada	43 47N	280 44E	+55.0	347.0
Fr	Fredericksburg, Virginia	38 12N	282 38E	+49.6	349.9
Am	Amberley, New Zealand	43 09S	172 43E	-47.7	252.5
K Index					
72469	Boulder, Colorado	40 08N	105 14W	+49.0	316.5
25602	College Observatory, Fairbanks, Alaska	64 52N	147 50W	+64.6	256.5
71816	Goose Bay, Labrador, Canada	55 20N	60 30W	+60.5	11.9
72712	Loring AFB, Maine	46 57N	67 53W	+58.5	1.5
03655	RAF Upper Heyford, England	51 56N	1 15W	+50.7	79.1
Q Index					
SOD	Sodankyla, Finland	67 22N	26 38W	+63.4	108.9

*From Prochaska³

K and K_p is large in 09-18 UT interval. Such a systematic difference leads to a time dependent relation between K and K_p.

To emphasize the large diurnal variation for a single station Q index, the hourly averages and average $\pm\sigma$ levels for Sodankyla for the same time period are shown in Figure 3 by the dotted lines. The Q index scale is basically the same as the K_p scale, with increments in steps of 1. The average curve of the Q index shows a minimum of 1 around 07-10 UT and a maximum of 2.3 around 22-00 UT. The average $\pm\sigma$ curve also has a maximum and a minimum at the same times. The two curves exhibit a large diurnal dependence both in the average and the variation

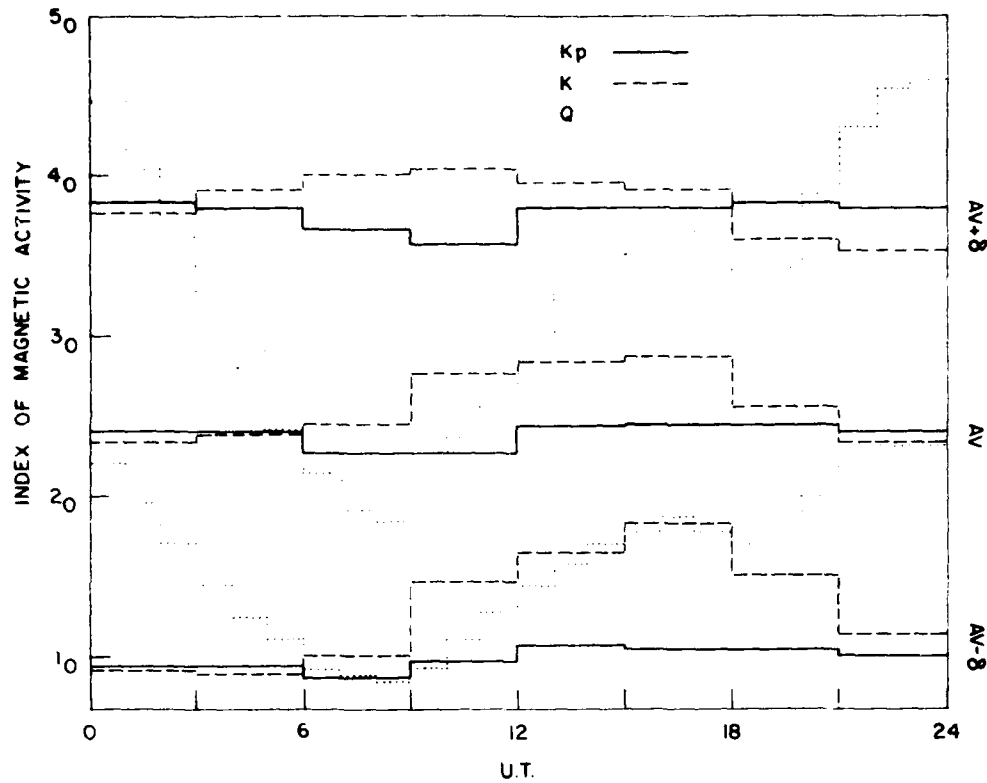


Figure 3. Diurnal Variation of K_p, K, and Q Indices

(σ level) of the Q index. To determine the relation between Q and K_p, or Q and K, the measurements must be restricted to the period 22-02 UT, when the statistical oval is closest to the Sodankyla station.

For estimating the extent of diurnal effects, an average least squared deviation straight line fit (for a possible failure of reciprocity, see Ref. 4) was obtained among K, K_p and Q for each hour. The results of these hourly dependencies are presented in Table 3. Section A presents a correlation between Q and K_p. Section B presents the correlation between Q and K. Section C presents the correlation between K_p and K. In Section C the correlations are for every 3 hours whereas in Sections A and B these are hourly values. In comparing K and K_p with hourly values of Q, it is assumed that the 3-hour indices are valid in each 1-hour sub-interval.

In each section the first column presents the interval of the day and the second column presents the correlation coefficient. The last two columns present the

Table 3. Summary of Correlation Analysis

Correlation Between (y and x)									
Section A					Section B				
Q and K _P		Slope m		Intercept c	Q and K		Slope m		Intercept c
UT Interval	Correlation Coefficient	UT Interval	UT Interval	Correlation Coefficient	UT Interval	UT Interval	Correlation Coefficient	UT Interval	Correlation Coefficient
0	0.775	1.56	-1.78	0	0.810	1.57	-1.74	0.01-0.13	0.846
1	0.801	1.43	-1.72	1	0.841	1.44	-1.68	0.14-0.16	0.872
2	0.791	1.30	-1.68	2	0.831	1.31	-1.62	0.06-0.08	0.884
3	0.765	1.14	-1.52	3	0.781	1.07	-1.37	0.06-0.12	0.853
4	0.773	1.00	-1.41	4	0.808	0.94	-1.27	0.12-0.15	0.846
5	0.759	0.90	-1.30	5	0.805	0.84	-1.16	0.15-0.18	0.835
6	0.759	0.82	-1.10	6	0.779	0.75	-1.13	0.18-0.21	0.814
7	0.790	0.72	-0.98	7	0.781	0.67	-1.04	0.21-0.26	0.876
8	0.778	0.68	-0.82	8	0.771	0.63	-0.98	Highest	0.884
9	0.713	0.84	-1.26	9	0.697	0.85	-1.70	Lowest	0.814
10	0.762	0.67	-1.36	10	0.743	0.90	-1.90		
11	0.767	1.11	-1.53	11	0.748	1.12	-2.11		
12	0.745	1.17	-1.68	12	0.723	1.45	-2.94		
13	0.788	1.24	-1.60	13	0.761	1.53	-3.02		
14	0.776	1.31	-1.76	14	0.746	1.63	-3.20		
15	0.772	1.35	-1.77	15	0.747	1.78	-3.60		
16	0.780	1.26	-1.53	16	0.774	1.71	-3.31		
17	0.746	1.22	-1.44	17	0.704	1.65	-3.21		
18	0.723	1.14	-1.38	18	0.684	1.54	-2.53		
19	0.743	1.21	-1.46	19	0.707	1.62	-2.66		
20	0.741	1.36	-1.63	20	0.712	1.85	-3.01		
21	0.738	1.32	-1.70	21	0.743	1.77	-2.18		
22	0.764	1.58	-1.72	22	0.774	1.85	-2.26		
23	0.766	1.62	-1.83	23	0.733	1.91	-2.40		
Highest	0.801	1.62	-0.92	Highest	0.841	1.91	-0.98		
Lowest	0.713	0.40	-1.83	Lowest	0.684	0.63	-3.60		

From 22-02 UT Q = 1.5 K_P - 1.7

slope and the intercept of the empirical least squares straight line fit. The last two lines list the highest and the lowest values respectively for correlation coefficient, slope and the intercept. Table 3 (and Figure 3) show a strong diurnal change in the relations among K, K_p and Q.

The magnitudes of the correlation coefficients from Table 3 are plotted in Figure 4. In Figure 4 the abscissa is the time in UT and the ordinate is the correlation coefficient. The continuous histograms are for K vs K_p. The dashed histograms are for K_p vs Q and the dotted histograms are for K vs Q.

For K vs K_p the correlation is high in all intervals, but dips slightly between 18 and 21 UT. The results show that K tracks K_p for most of the hours, but this tracking is somewhat degraded in the same 18-21 UT sector.

The correlation between K_p and Q is always ≥ 0.7 showing that these variations are also well correlated. The effect of the diurnal variation of Q on the actual relationship will be considered later.

The correlation between K and Q is ≥ 0.68 . The significance of the variations is seen in the next figure.

Figure 5 shows the variation with UT of the slopes of the empirical straight line fits from Table 3. The corresponding range of modulation (highest minus the lowest slope) is shown on the right hand side. The modulation is least for K_p vs K and is highest for K vs Q.

Before interpreting the meaning of slope and its variation, it should be remembered that K and K_p have identical scales ranging from 0 to 9_o in steps of 1/3. The Q scale ranges from 0 to 11 in steps of 1. K and K_p are indices over an interval of 3 h. The Q index has a much finer resolution (compared to that of K or K_p) of 15 min. A difference in the distribution of the stations contributing to the respective indices (Figure 2) must also be taken into account.

Magnetic disturbances are known to occur most often in the magnetic midnight sector. Therefore any reference to time should be with respect to magnetic midnight. However, each station in the AFGWC magnetic network has a different magnetic local time for the same Universal Time. Therefore, it is convenient to use UT in the following discussions.

The slope of K_p vs K is < 1 in the 03-09 UT interval, showing that the response of K to magnetic activity is stronger than the response of K_p in this period. In the 15-21 UT sector, the slope of K_p to K is highest. This shows that the response of K to increased magnetic activity has become weaker in this period than the response of K_p. The variation of slope during a period of 24 h shows a systematic diurnal change in the relationship between K and K_p. The 03-09 UT interval when K is stronger than K_p corresponds to the magnetic midnight in the American sector, where four of the five stations that measure the K index are located. In the 15-21 UT interval the American sector is farthest from the auroral oval; therefore K is weaker than K_p.

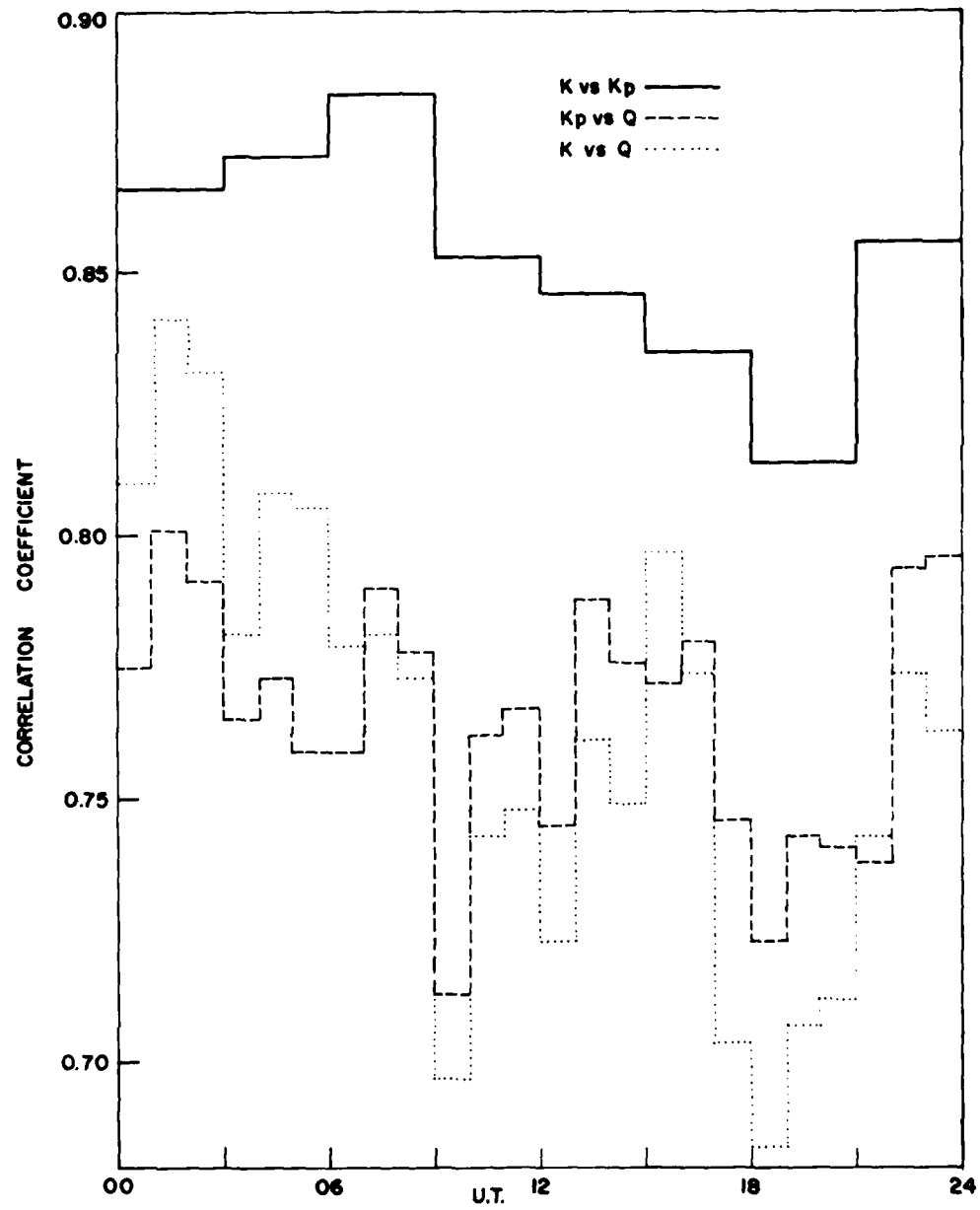


Figure 4. Dependence of the Correlation on UT for (a) K_p vs K , (b) K vs Q ,
(c) K_p vs Q

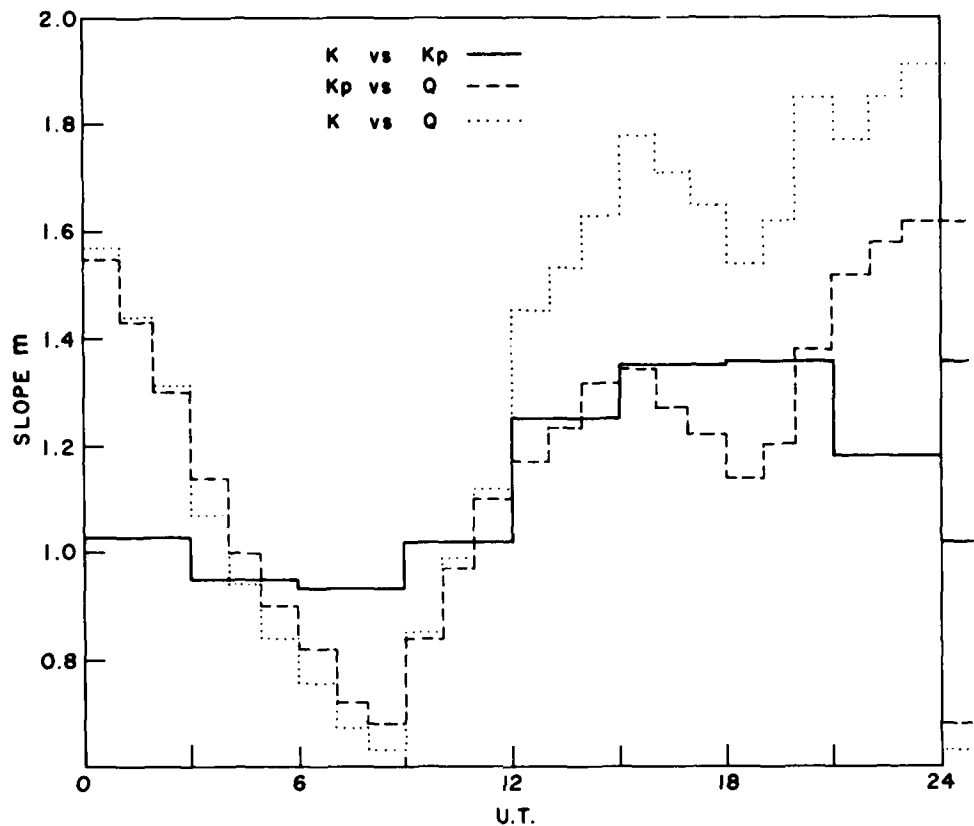


Figure 5. Dependence of Multiplication Factors (Slope) on UT for (a) Kp vs K,
(b) K vs Q, (c) Kp vs Q

The Q index also shows diurnal variation, caused by the movement of Sodankyla towards and away from the auroral oval as the earth rotates. Figure 1 shows how the station is closest to the oval near 22-00 UT and farthest around 07-09 UT. The Q index is most accurate from 22 to 00 UT and least useful from 07 to 09 UT. A relation between Q and Kp is valid only during periods when both Q and Kp are accurate.

In Figure 5, the slope of Kp vs Q reaches its highest value between 23 and 01 UT, the time period during which the Q index is most accurate. The slope reaches its minimum value between 07 and 09 UT when Sodankyla is farthest from the oval and the Q index least accurate. The overall modulation factor is 2.4, from this data base of 39 months. This factor agrees well with the previous study¹ which showed a modulation factor of 2.6 from another data base of 4 years.

Therefore, the slope given in Table 3 for the 22-02 UT interval, when the Q index is most accurate, will be used in the empirical relations to be derived later.

The variation in the slope of K vs Q is caused by two factors:

- (i) the diurnal variation in the response of Q (measured at Sodankyla) to auroral oval activity;
- (ii) a minor diurnal variation in the response of K with respect to the K_p index, caused by the derivation of K from stations mainly in the American sector.

This combination produces a modulation of a factor of 3.1 in the slope. This extreme difference in the response of K to K_p and Q around 06-08 UT, compared to the response around 20-23 UT is due mainly to the weak response of Q to auroral activity. The response is weak because Sodankyla is farthest from the auroral oval at magnetic noon.

Figure 6 is a plot of the extreme values of K vs K_p from Table 3. These occur around 06-09 UT and 18-21 UT. In the figure, K is plotted along the abscissa and K_p along the ordinate. The solid line shows the slope for the 06-09 UT interval and the dashed line for the 18-21 UT interval. For comparison, the dash-dot line has been drawn with a slope of 1 (45°), offset from the origin to account for the fact that K = 0_o is absent. Comparison of the lines shows that K and K_p are in excellent agreement from 06 to 09 UT. Also, K and K_p are in excellent agreement from 18 to 21 UT in the magnetic activity range 1₋ to 2₊. For K \geq 3, the difference between K and K_p is successively larger. These systematic changes are superimposed on the local fluctuations in K that occur because four of the five stations are in a narrow sector.

This information can be used to improve the derivation of the Q index from the AFGWC K index. The data from the period 22-02 UT, the period of highest correlation between K_p and Q, showed (from Table 3)

$$Q = 1.5 K_p - 1.7 \quad (2)$$

K_p can be written as a function of K of the form

$$K_p = AK + B \quad (3)$$

where the slope A and the intercept B are time dependent empirical constants listed in Table 3.

Combining Eqs. (2) and (3) gives

$$Q = A_1 + B_1 K \quad (4)$$

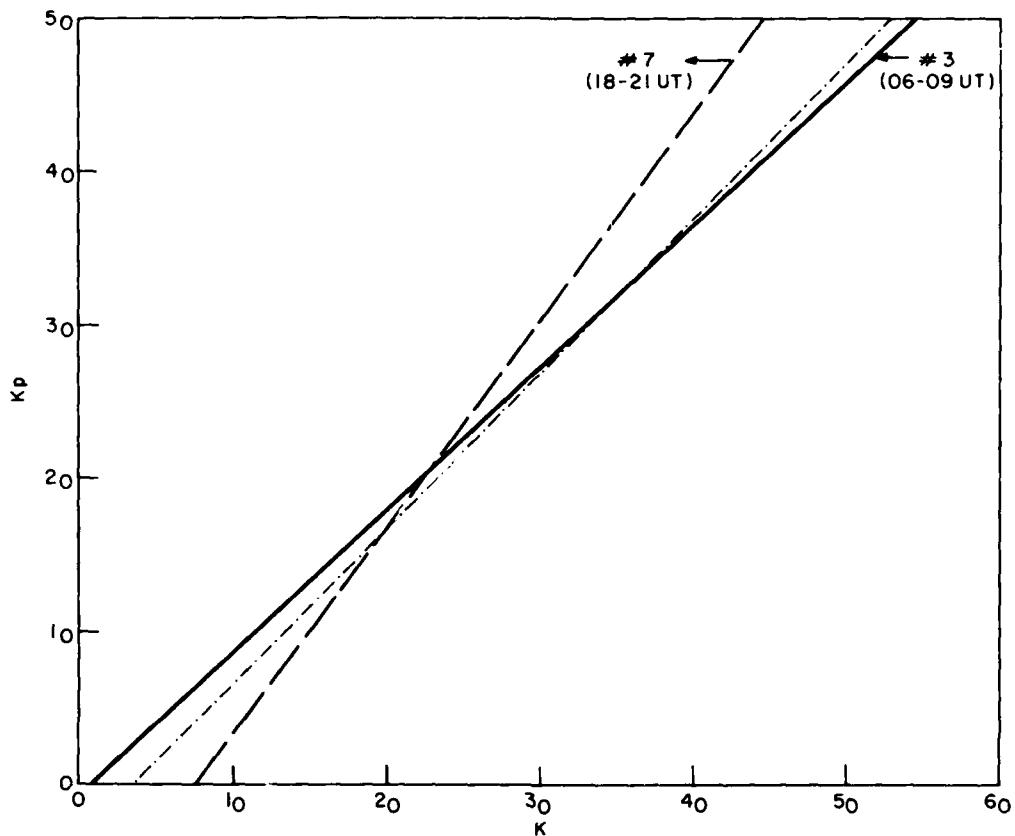


Figure 6. Relations Between K_p and K for 06-09 UT and 18-21 UT Intervals

where

A_1 is a time dependent constant

B_1 is a time dependent slope or multiplying factor of the index K ,
and

K is the magnetic activity index determined by the AFJWC network.

The empirical time dependent constants A_1 and B_1 computed from Table 3 are presented in Table 4. The first column in Table 4 lists the time interval for K . The next two columns present the slope A_1 and the intercept B_1 for the empirical relation. The average values of A_1 and B_1 are listed in the last line of the table. The slope A_1 changes by 60 percent between intervals 3 and 7. For the same intervals the intercept changes by a factor of 2.

Table 4. Empirical Time Dependent Factors for Conversion of K to Q

$Q = A_1 K + B_1$		
where A_1 and B_1 are time dependent terms		
Time Interval of K UT	Slope A_1	Intercept B_1
00-03	1.54	-1.7
03-06	1.43	-1.6
06-09	1.40	-1.8
09-12	1.53	-2.5
12-15	1.87	-3.3
15-18	2.02	-3.9
18-21	2.03	-3.2
21-00	1.77	-2.2
Average	1.70	-2.5
$Q = 1.5 K_p - 1.7$		

4. CONCLUSIONS

The K index shows a skewed distribution with respect to the Kp index. At the lower end K is 1/3 unit larger than Kp and at the upper end K is 1/3 unit smaller than Kp. In addition K shows a diurnal variation. These shortcomings in the data are corrected by deriving empirical relations between K and Kp.

An empirical time dependent relation between Q and K has been determined for specifying the auroral ionosphere from AFGWC K observations. K tracks Kp very well in the 03-09 UT interval, whereas the relationship between the two is somewhat degraded in the 18-21 UT interval. Due to the diurnal motion of a magnetometer station with respect to the auroral oval, caution is required in a direct use of the Q-index from a single station, like Sodankyla. The overwhelming consideration is the time dependence of K due to a limited network of stations. Statistically, the differences between K and Kp are negligible for $K = 1_-$ to 2_+ . The differences, which are time dependent, become successively larger for $K \geq 3$. This time dependence can be corrected by use of empirical factors in Table 4 for a determination of the Q index for specification of the auroral ionosphere from K.

The best longterm approach is to determine and correct the causes (possibly algorithms of K) to eliminate the systematic discrepancies between K and Kp.

Dandekar¹ used a four year data base for studying the Q-index behavior from Sodankyla. Dandekar² has shown that for ± 3 hours around CG midnight, the equatorward precipitation boundary determined from the continuous (diffuse) aurora is within 1° of the latitude predicted from the Feldstein/Starkov⁷ analysis of $Q > 2$. Dandekar's results based on a larger data base are summarized in Appendixes A and B for comparison with results of the present study with a smaller data base.

Appendices A and B consolidate the new information relating to magnetic activity indices relevant to the ERS data analysis.⁸

-
7. Starkov, G.V. (1969) Analytical representation of the equatorial boundary of the auroral oval zone, Geomagn. Aeron., (Eng. ed), 9:614.
 8. Gassman, G.J. (1973) Analog Model 1972 of the Arctic Ionosphere, AFCRL-TR-73-0151, AD 762 280.

References

1. Dandekar, B.S. (1979) Magnetic Disturbance Statistics from a Single Station Q Index Applied to an Actual OTH-B Radar Situation, AFGL-TR-79-0296, AD A084 808.
2. Dandekar, B.S. (1979) Study of the Equatorward Edge of the Auroral Oval from Satellite Observations, AFGL-TR-79-0010, AD A072 997.
3. Prochaska, R. D., Capt., Geomagnetic Index Calculation and Use at AFGWC, AFGWC/Tn-80/002.
4. Spiegel, M. R. (1969) Theory and Problems of Statistics, Schaum Publishing Co., New York, p. 229.
5. Bartels, J., and Fukushima, N. (1956) Ein Q-Index für die Erdmagnetische Aktivität in Viertelstündlichen Intervallen, Abhandl. Akad. Wiss. Gottingen, Math-Phys. Klasse, Sonderheft-2.
6. Feldstein, Y.I. (1963) On the morphology of auroral and magnetic disturbances at high latitudes, Geomagn. Aeron. 3:183.
7. Starkov, G. V. (1969) Analytical representation of the equatorial boundary of the auroral oval zone, Geomagn. Aeron., (Eng. ed), 9:614.
8. Gassman, G.J. (1973) Analog Model 1972 of the Arctic Ionosphere, AFCRL-TR-73-0151, AD 762 280.

Appendix A

Determination of Q (or Kp) From Photometric Auroral Observations

For an effective operation of the experimental radar system, one needs ionospheric maps, to provide an assessment of the environment in which the radio waves must propagate.

One of the important parameters needed for a generation of ionospheric maps of the surveillance area, is the magnetic activity index Kp or Q. The conventional methods are unable to yield values of Kp or Q on a real time basis.

Gassmann suggested the use of the equatorward boundary of diffuse aurora as a real time indicator for the magnetic activity index Q.⁸ In the absence of a statistical analysis of diffuse aurora, he further suggested the use of the Starkov equation⁷ for determining the effective Q index - Q_{eff} from the observed equatorward boundary of the diffuse aurora in the magnetic midnight meridian.

Starkov⁷ fitted an empirical circle to the Feldstein oval⁶ of discrete auroral arcs. The resulting equation is given by:

$$\theta_{eq} = 72 - 0.9 Q - 5.1 \cos(t - 12) \quad (A1)$$

where

θ_{eq} - is the equatorward latitude in geomagnetic coordinates of the discrete aurora (on the magnetic midnight meridian)

Q - is the magnetic activity index Q, and

t - is (0° for the magnetic midnight meridian) the time in degrees measured eastwards from the magnetic meridian.

Dandekar² studied the relationship between magnetic activity and the equatorward edge of diffuse aurora observed by wideband spectral photometers aboard the satellites of the Defense Meteorological Satellite Program. For the northern hemisphere, Dandekar derived empirical relations from a large data base of 1972-1976.

$$\theta_{eq} (\text{diffuse aurora}) = 71.2 + 1.4 K_p - 2.7 \cos(t-13) \quad (A2)$$

and

$$\theta_{eq} (\text{diffuse aurora}) = 69.2 + 1.0 Q - 2.6 \cos(t-5) \quad (A3)$$

where

K_p - is the planetary index of magnetic activity, and other terms are the same as in Eq. (A1).

One can solve Eqs. (A1) - (A3) and determine the relationship between Q , discrete arcs, K_p , and Q , diffuse aurora. For the sake of convenience the equatorward boundary of the aurora determined from the preceding equations is shown in Figure A1. Figure A1 consists of three sections. In each section the abscissa is the index of magnetic activity and the ordinate is the geomagnetic latitude of the equatorward edge of the aurora.

The section at the top presents the dependence of the equatorward edge of the diffuse aurora (from DMSP pictures) on the magnetic activity index K_p . The middle section shows the dependence of this boundary on the magnetic activity index Q . The last section at the bottom shows the dependence of the equatorward boundary of the discrete auroral arcs (Feldstein oval) with Q . The equations presenting the respective relationships are indicated at the right hand top corner of each section. From these figures one can determine the latitudinal location of the appropriate feature in the magnetic midnight sector if the level of the index of magnetic activity is known.

On the other hand, for ionospheric mapping one can use these graphs for obtaining the essential parameter Q or K_p from the equatorward edge of the diffuse aurora seen in the DMSP pictures.

In assessing the ionospheric environment for the radar operation, workers have used diffuse auroral boundary/discrete auroral boundary and K_p/Q as inputs in their computation procedures. One can determine the interrelations among these parameters by using the graphs in Figure A1. For this purpose the values of K_p (and Q), are read at each latitude and are plotted in Figure A2.

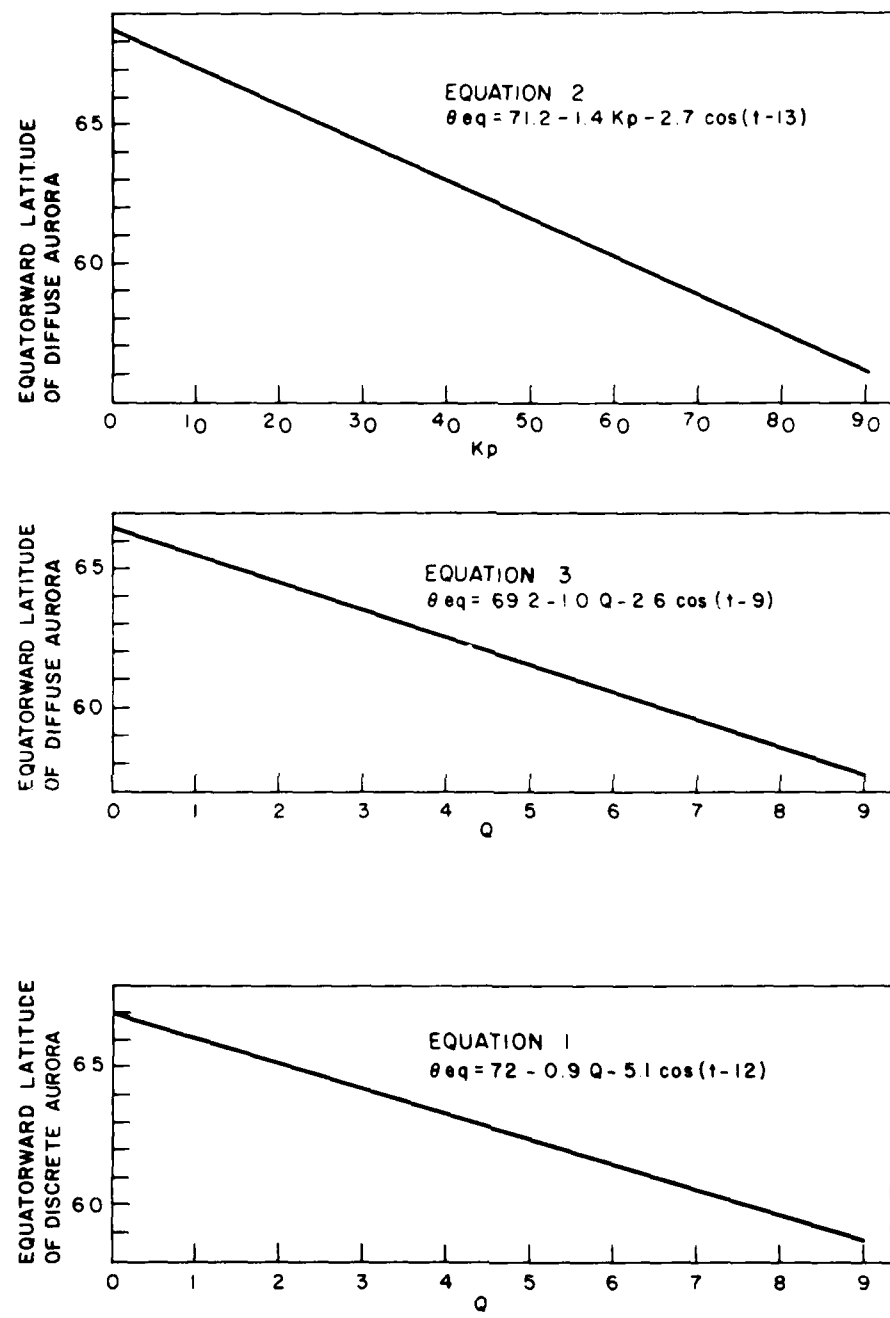


Figure A1. Location of Equatorward Edge of Aurora vs Kp and Q Indices

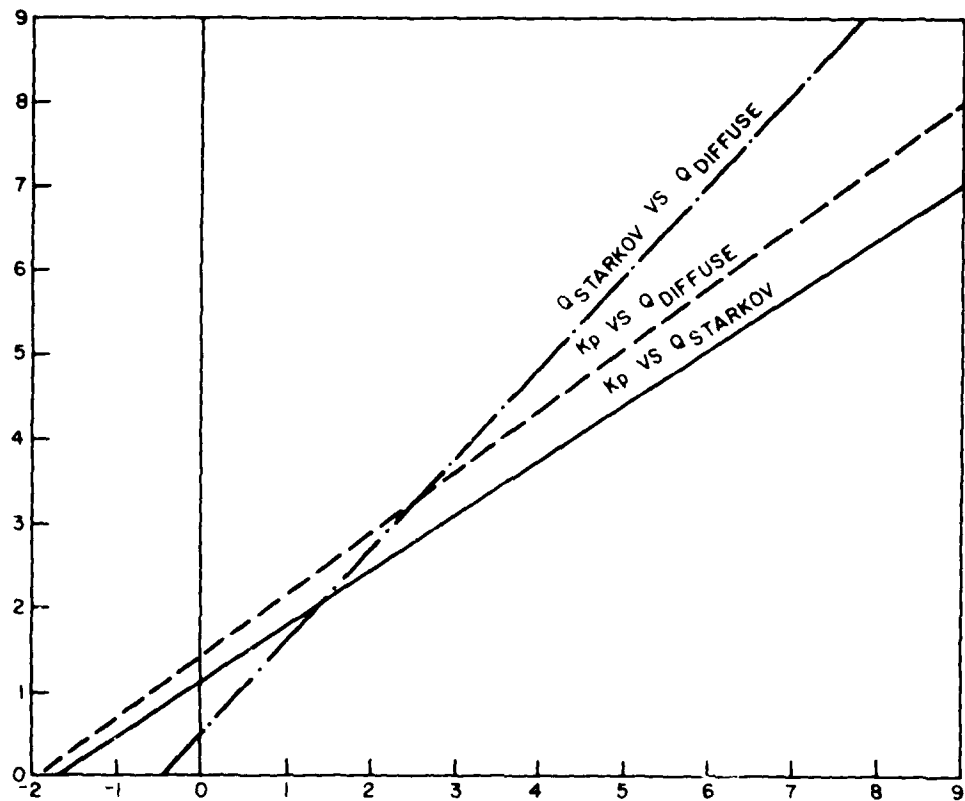


Figure A2. Relations Among Magnetic Activity Levels and Auroral Locations

In Figure A2 each curve is labeled by two parameters. The beginning parameter refers to the scale of the ordinate (y-axis) and the end parameter presents the scale for the abscissa (x-axis). For example, the top curve shows that, the equatorward boundary of the diffuse aurora at magnetic activity level $Q = 6$, is attained by the discrete aurora when Q reaches (the higher) level 7. This is consistent with the fact that the discrete aurora usually lies polewards of the diffuse aurora. As another example, the dashed curve shows that, the magnetic activity $Q = 0$ is approximately equal to $K_p = 1_+$ (1.33). The difference in slopes and the cut-off of the curves suggest that one should be careful in using appropriate scales for the level of magnetic activity used in the generation of the ionospheric maps.

Appendix B

Relationship Between K_p and Q_{SOD}

For determining a relationship between K_p , the planetary index of magnetic activity and Q_{SOD} , the magnetic activity index Q from the high-latitude station Sodankyla (Geog. Lat. 67.4° N, Geog. Long. 24.7° E, Corrected Geomagnetic Lat. 63.9° N, Corrected Geomagnetic Long. 108.5° E), the respective data for the years 1965, 1968, 1971 and 1974 were used.

A previous study¹ of the Q index data from Sodankyla showed a systematic diurnal variation due to the change in relative distance between the oval boundary and the station as a function of time of day. This systematic diurnal variation was eliminated by computing empirical detrending factors for the Sodankyla station.

The K_p index is available at intervals of 3 hours, whereas the Q index is available at intervals of 15 minutes. From these data a least-squares straight line fit between K_p and Q_{SOD} was obtained for each hour, from both the original Q index data and also from the detrended Q index data. These results are summarized in Table B1.

In the table the relationship is of the form $Q = m K_p + c$ where m and c are computed as a least squares fit. In the table the first column lists the year for which the data were used. The second column gives the nature of data. As the diurnal variation shows a systematic maximum and minimum, the hour of the maximum or minimum in the original data is listed in the next column. The next three columns present the correlation coefficient, the slope m , and the offset (cutoff) c for the empirical fit. The table shows that the original data exhibits a maximum

Table B1. Relationship Between K_p and Q_{SOD}

Year	Sodankyla Data	Time UT	Correlation Coefficient	Slope m	(Cut Off) Offset C	Ratios of	
						m's	C's
1965	Original	07 22	0.652 0.768	0.369 1.125	0.22 0.68	3.05	3.09
	Detrended	All	0.690	0.939	0.57		
1968	Original	07 22	0.706 0.894	0.570 1.497	0.44 1.00	2.63	2.27
	Detrended	All	0.727	1.464	0.80		
1971	Original	05 22	0.644 0.784	0.483 1.302	0.24 0.72	2.72	3.00
	Detrended	All	0.664	1.257	0.47		
1974	Original	08 23	0.735 0.800	0.603 1.545	0.47 1.36	2.56	2.89
	Detrended	All	0.702	1.290	0.69		
Average	Original	At min At max	0.684 0.792	0.506 1.367	0.34 0.94	2.74	2.81
	Detrended	All	0.702	1.238	0.63		

$$Q = 1.4K_p - 0.9 \quad \text{Or} \quad K_p = 0.73 Q + 0.66$$

and a minimum in the diurnal variation around 22 and 07 UT respectively. The correlation between K_p and Q is > 0.6 at all times. The slope indicates that the relation is stronger when the station is closer to the oval, and is weaker when the station moves away from the oval, when original Q index data are used. For each year the ratio of the slope (m) at the maximum (22 UT) with respect to that at the minimum (07 UT) is computed. These are presented in the last two columns respectively. For each year the respective ratios (of m 's and c 's) are approximately equal. The equality of these ratios indicates that the empirical detrending terms would be multiplying/dividing factors and could not be addition/subtraction type terms. The slopes of detrended data when compared with the maxima of original data are in good agreement. The close agreement shows that the empirical detrending factors effectively remove the systematic diurnal variation. The averages from each of the 4 yr are listed in the middle section of the table. From the 4 yr data base the magnitude of the highest detrending factor is 2.8 (for data around 07 UT). The empirical equations are presented at the bottom section of the table. The empirical relations will enable the determination of a Q index from the K_p index. The Q index data are needed in the ionospheric models for predicting or estimating the locations of the auroral oval, auroral E layer and the F layer trough features.

